www.rericjournal.ait.ac.th

Modelling of a Solar Ejector Cooling System using CPV Collector

Carlo Renno*,[1] and Olga Di Marino*

ARTICLE INFO

Article history:
Received 21 December 2023
Received in revised form
16 May 2024
Accepted 24 June 2024

Keywords:
Cooling
Concentrating photovoltaic system
Ejector
Exergoeconomic analysis
Model

ABSTRACT

The aim of the paper is the modelling of an ejector cooling system driven by a concentrating photovoltaic (CPV) collector; a single-stage ejector is used. The CPV modules represent a technological innovation allowing to obtain electric energy with efficiency and temperature values higher than traditional photovoltaic systems. Hence, the thermal energy can drive processes such as solar cooling. On the contrary, the CPV systems need a major maintenance and their use is preferable where the climate is not wet. The model input data are the outdoor temperature and solar irradiation values of some Italian sample cities. The model output data are represented by solar collector efficiency, evaporation power, COP and $COP_{overall}$. Moreover, an exergoeconomic analysis is carried out to compare the product cost of an ejection cooling system driven by CPV module (CPV/ECS) and a traditional electric heat pump (EHP). Finally, a SPB of 7.4 years is obtained adopting a CPV/ECS instead of EHP and, using also the electric energy of CPV system to match the domestic user electric requirements, a further saving is possible with a SPB equal to 5.2 years.

1. INTRODUCTION

Climate change is one of the most urgent and complex challenges that humanity faces in the 21st century for the survival and development of humankind and requires a transition to a low-carbon energy system [1]. Approximately 40% of global CO_2 emissions come mainly from the energy production sector [2]. Moreover, the energy demand for building cooling is increasing due to population growth and economic progress, especially in emerging countries [3]. It is estimated that by 2050, energy demand for cooling will be tripled and it will be about 37% of global electricity demand [4]. The use of solar energy, with its wide range of applications, appears to be promising for refrigeration purposes [5]. Recently, solar-powered refrigeration cycles have received significant attention among alternative air-conditioning and cooling systems, representing interesting possibilities for reducing energy consumption, especially in locations with strong solar potential [6]. These systems are characterised by high reliability, simple maintenance and low operating costs. Moreover, they can play a significant role in reducing greenhouse gases by avoiding the use of environmentally harmful refrigerants used in mechanical vapour compression air conditioning systems. In literature [7], there are different designs of solar-driven ejector refrigeration systems: single-stage, multi-stage, with booster or compressor, solar-driven combined ejector and absorption (or adsorption) systems. Single-stage ejector refrigeration systems are above all studied [8] and several experimental plants have been realized with different refrigerant fluids [9]-[10]. In [11] a solar cooling system is developed using R141b that allows achieving a high COP equal to about 0.5.

In [12], a solar-powered ejector cooling system is employed to reduce the energy consumption of an inverter-type air conditioner. In [13] a 1-D analysis of the ejector's performance during critical operation is conduced. An experiment using 11 ejector and R141b as the working fluid is carried out to demonstrate the accuracy of the prediction. In [14] a solar-powered refrigeration system that uses water or natural refrigerants at low temperatures as working fluid, is developed. The system has a COP equal to about 0.3.

It is difficult to keep the system running at optimum conditions because of variable working conditions as, for example, low insolation; hence, multi-stage systems can be used [9]. A booster can be adopted to increase the COP [15]. The COP of the ejector-based refrigeration system is relatively low, limiting its industrial applications [7]. The use of variable geometry ejectors in refrigeration systems can lead to optimal performance in a wide range of operating conditions [16].

The solar ejector cooling system performances depend also on the type and efficiency of collector used [17]-[18]. To satisfy electrical and thermal loads, the PV module is advantageous from an economic and environmental perspective. Hybrid PV/T collectors are above all not concentrating [19] and the thermal energy is available at low temperatures (40÷60°C), suitable for

*Department of Industrial Engineering, University of Salerno, Via Giovanni Paolo II 132, 84084 Fisciano (Salerno), Italy.

[1]Corresponding author:
Tel: +39 089 964327.
Email: crenno@unisa.it.

domestic water and space heating but inadequate for applications at higher temperatures such as solar cooling. On the contrary, a concentrating photovoltaic thermal system (CPV/T) allows to produce electric energy with high efficiency and to obtain higher temperatures even above 100°C. In the CPV/T module, the thermal energy is a low cost product that can lead to competitive solar cooling solutions also for domestic applications in hot regions with low humidity [20]-[21]. In [22] a CPV/T system with absorption cooling is studied. To work efficiently, solar-driven ejector cooling systems require temperatures higher than 70°C and obtainable with CPV/T modules. Hence, the main aim of the paper is the determination of a model able to verify how an ejector cooling system works with a CPV/T collector in some Italian cities whose outdoor temperatures and solar irradiation values [23] represent the model input data. The ejector allows to obtain cooling at almost zero cost without moving parts, and the CPV/T collector assures electric energy and higher working fluid temperatures [24]. The model output data are collector efficiency, evaporation power, COP, $COP_{overall}$ and ejector entrainment ratio. A thermoeconomic analysis is presented to compare the system proposed with a traditional cooling system.

2. SYSTEM DESCRIPTION

2.1 Ejector Cooling System

The ejector cooling system consists of concentrating photovoltaic thermal module (CPV/T), water pump, generator, separator, ejector, condenser, evaporator, expansion valve and another pump (Figure 1). The solar radiation is incident on a CPV/T collector heating water that can reach temperatures between 60°C and 120°C. In the generator the water exchanges heat with the HFO-1336mzz-Z refrigerant fluid [25] that reaches conditions of dry saturated vapour (g) and enters the ejector. The refrigerant fluid successively enters the condenser and reaches conditions of saturated liquid (3). The refrigerant mass flow rate is divided into two parts by a separator, the primary fluid returns to the generator, the secondary fluid crosses the expansion valve reaching conditions of saturated vapour (4); finally, the refrigerant fluid leaves the evaporator in conditions of dry saturated vapour (1-e).

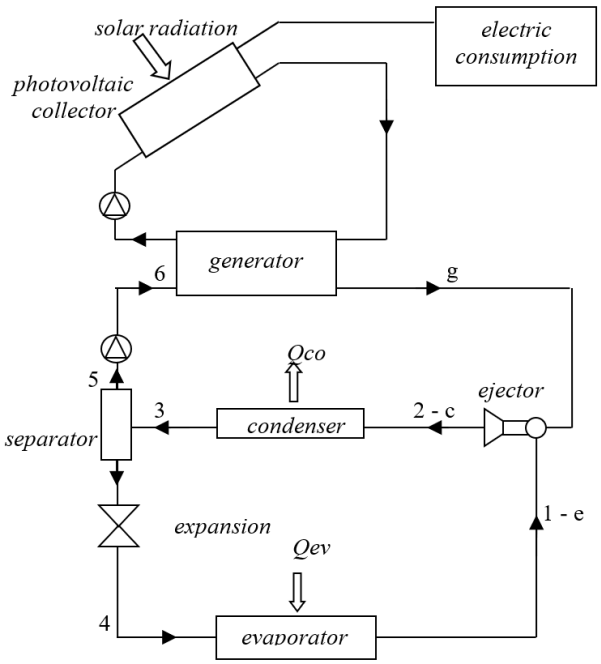

Fig. 1. Plant scheme.

2.2 CPV/T collector

The CPV/T systems present problems if the climate is wet because of high levels of diffuse light and intermittent periods of direct sunlight. The reflecting surfaces inclination is determined to maximize the radiation reflected on the tubes containing the working fluid. The concentrators generally used are: parabolic dish, parabolic trough or heliostat field. The CPV module presents high operating costs due to the electronic control system to chase direct radiation and the optic instruments protection. The plant analyzed presents a CPV/T collector able to produce electric and thermal energies; the CPV module is based on triple junction cells with η_{el} of about 25% [26] and peak power of 0.15 kW_p. The CPV cells are located on a plate that transfers heat to water (Figure 2); other fluids are used for temperatures above 100°C. A concentration ratio of a few hundreds and optical efficiency (η_{op}) equal to 0.85, typical values for dish concentrators [27], have been chosen. Other types of CPV modules determine different concentration ratio and η_{op} values, and the analysis can be modified. As for the radiation power ($\dot{Q}_{rad}$) incident on the collector, the output electric power ($\dot{L}_{el}$) is equal to:

$$\dot{L}_{el} = (\dot{Q}_{rad}\eta_{op}\eta_{pv} - \dot{Q}_{par})\eta_{inv} \quad (1)$$

where η_{pv} and η_{inv} are respectively the PV module and inverter efficiencies, and $\dot{Q}_{par}$ is the parasitic power equal to about 2% of the intercepted radiation power. The CPV cells efficiency varies with the concentration ratio and cell temperature values according to [22]. The thermal power absorbed by the collector is equal to:

$$\dot{Q}_t = \dot{Q}_{rad}\eta_{op}(1-\eta_{pv}) \quad (2)$$

The coolant heated leaves the CPV/T module and reaches the generator (Figure 1) where provides thermal energy to the ejector cooling system.

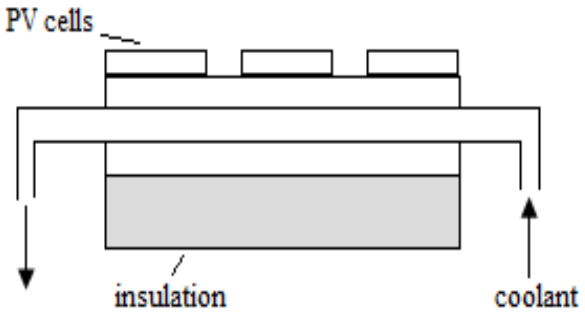

Fig. 2. Scheme of the CPV/T collector.

2.3 Ejector

The ejector consists mainly of nozzle, mixing chamber and diffuser (Figure 3). The nozzle and diffuser have a converging/diverging geometry. Diameters and lengths of nozzle, mixing chamber and diffuser, define the ejector performances. The ejector capacity depends on the motive (primary) and entrained (secondary) flow rates, whose sum gives the compressed mass flow rate. Single-stage ejector with a mixing at constant-pressure is considered in this paper to increase the pressure. The motive flow enters the ejector converging part (Figure 3: section *g*) at subsonic velocity, and its pressure decreases and its velocity increases.

The stream reaches the sonic velocity at the nozzle throat, where its Mach number is equal to one; the cross-section area increase of the nozzle diverging part determines a pressure decrease and a velocity increase under supersonic conditions. At the nozzle outlet (*1*) the motive flow pressure becomes lower than the evaporation pressure. The entrained flow, dragged by vapour that comes out of the nozzle at high speed, enters the ejector (*e*) where its velocity increases and its pressure decreases (*y*). The mixture goes through a shock inside the constant cross-section area of the diffuser. The shock is due to the condenser back pressure resistance that determines a mixture pressure increase and a velocity decrease under subsonic conditions (*s*). As the subsonic mixture emerges from the constant cross-section area of the diffuser, a further pressure increase occurs in the diffuser diverging section. The emerging fluid pressure is higher than the condenser pressure (*c*). COP depends on the cycle temperatures and irreversibility rates in the diffuser and nozzle and the two fluids mixing process at different velocity and shock wave.

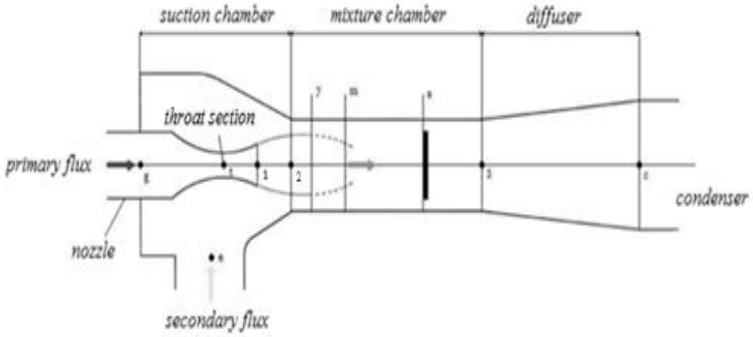

Fig. 3. Ejector.

3. MODELLING OF A CPV/ECS SYSTEM

3.1 Modelling

The mathematical model of an ejection cooling system driven by CPV module (CPV/ECS) has been implemented in Matlab [29]. The program consists of two parts: the first determines the CPV/T collector performances, the second evaluates the ejector cooling system performances. The refrigerant fluid properties values have been determined by means of Refprop (Version 8.0, NIST) [29]. As for the collector, the solar irradiation and outdoor temperature values of six Italian sample cities (Milano, Bologna, Firenze, Roma, Napoli, Palermo) [23] have been considered as model input data necessary to determine the output working fluid temperature and the efficiency of the collector in accordance with the equations reported in [21]. As for the performances determination of the ejector cooling system, the input data are: motive fluid pressure and temperature (T_g, p_g) and entrained fluid pressure and temperature (T_e, p_e), nozzle geometry (d_t,d_1), c_p, R and γ. The output data are: ejector entrainment ratio (ω), condenser inlet temperature (T_{cond}) and secondary fluid mass flow rate ($\dot{m}_s$), evaporation power Q_{ev}, COP and $COP_{overall}$ (Figure 4). For different ejector output section values, the program verifies if both fluids are in choking conditions and if there are malfunction conditions.

3.2 Equations

The equations of the nozzle, mixing and diffuser sections of the ejector are: mass, energy, momentum equations and other auxiliary equations [13]. The shock and mixing at the ejector inlet are difficult matters; for this some exemplifying hypotheses are necessary:

ejector adiabatic inner wall, flow steady and isentropic inside the ejector, one-dimensional flow, primary and secondary fluids reach the ejector at zero velocity, negligible kinetic energy at the ejector outlet, two fluids mix with uniform pressure from y section to m section ($p_m=p_{sy}=p_{py}$), secondary flow reaches the choking condition at y section ($M_{sy}=1$), gas ideal with constant specific heats [30]. In order to consider the non-ideal process in the model, the effects of mixing and frictional losses are evaluated using in the isentropic relations some coefficients experimentally determined [30]. Some of the equations used to calculate flow properties and system performance have been adapted from [31], that provides a methodology for calculating the mess flow of the primary flow (Equation 3). This method takes into account the isentropic efficiency of the Laval nozzle, considering friction losses.

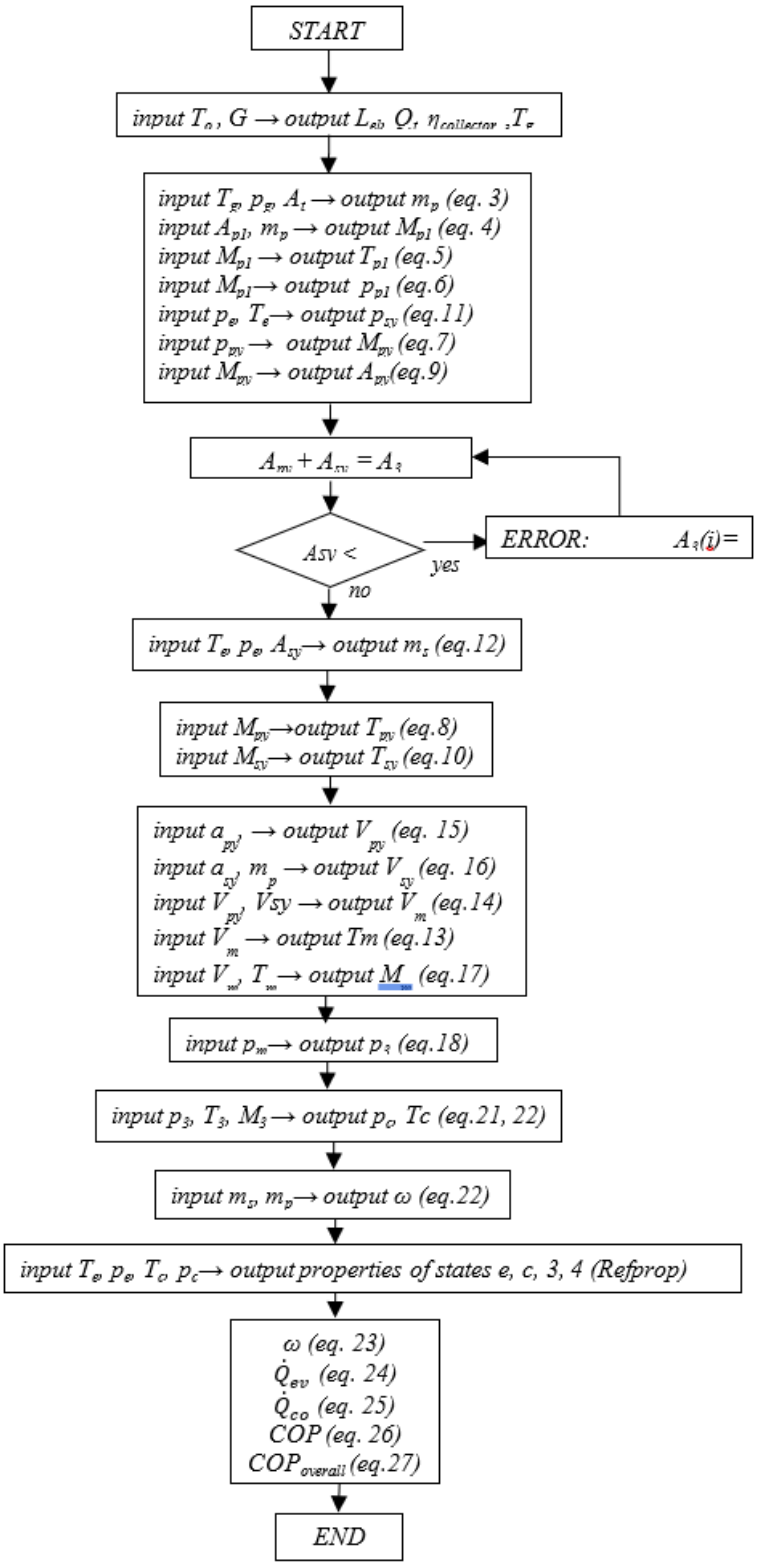

Fig. 4. Flowchart model.

Primary flow in the nozzle

$$\dot{m}_p = \frac{p_g A_t}{\sqrt{T_g}} \sqrt{\frac{\gamma}{R}\left(\frac{2}{\gamma+1}\right)^{\frac{\gamma+1}{\gamma-1}}} \sqrt{\eta_p} \tag{3}$$

$$\frac{A_{p1}}{A_t} = \frac{1}{M_{p1}}\left[\frac{2}{\gamma+1}\left(1+\frac{\gamma-1}{2}M_{p1}^2\right)\right]^{\frac{\gamma+1}{2(\gamma-1)}} \tag{4}$$

$$\frac{T_g}{T_{p1}} = 1+\frac{\gamma-1}{2}M_{p1}^2 \tag{5}$$

$$\frac{p_g}{p_{p1}} = (1+\frac{\gamma-1}{2}M_{p1}^2)^{\frac{\gamma}{\gamma-1}} \tag{6}$$

Primary flow from section 1 to y

$$\frac{p_{py}}{p_{p1}} = \left(\frac{1+\frac{\gamma-1}{2}M_{p1}^2}{1+\frac{\gamma-1}{2}M_{py}^2}\right)^{\frac{\gamma}{\gamma-1}} \tag{7}$$

$$\frac{T_g}{T_{py}} = 1+\frac{\gamma-1}{2}M_{py}^2 \tag{8}$$

$$\frac{A_{py}}{A_{p1}} = \frac{\frac{\phi_p}{M_{py}}\left[\frac{2}{\gamma+1}\left(1+\frac{\gamma-1}{2}M_{py}^2\right)\right]^{\frac{\gamma+1}{2(\gamma-1)}}}{\frac{1}{M_{p1}}\left[\frac{2}{\gamma+1}\left(1+\frac{\gamma-1}{2}M_{p1}^2\right)\right]^{\frac{\gamma+1}{2(\gamma-1)}}} \tag{9}$$

Secondary flow from inlet section to section y

$$\frac{T_e}{T_{sy}} = 1+\frac{\gamma-1}{2}M_{sy}^2 \tag{10}$$

$$\frac{p_e}{p_{sy}} = (1+\frac{\gamma-1}{2}M_{sy}^2)^{\frac{\gamma}{\gamma-1}} \tag{11}$$

$$\dot{m}_s = \frac{p_e A_{sy}}{\sqrt{T_e}} \sqrt{\frac{\gamma}{R}\left(\frac{2}{\gamma+1}\right)^{\frac{\gamma+1}{\gamma-1}}} \sqrt{\eta_s} \tag{12}$$

Flow mixed at section m before of the shock

$$\dot{m}_p\left(c_p T_{py} + \frac{V_{py}^2}{2}\right) + \dot{m}_s\left(c_p T_{sy} + \frac{V_{sy}^2}{2}\right) = (\dot{m}_p+\dot{m}_s)\left(c_p T_m + \frac{V_m^2}{2}\right) \tag{13}$$

$$\phi_m(\dot{m}_p V_{py} + \dot{m}_s V_{sy}) = (\dot{m}_p+\dot{m}_s)V_m \tag{14}$$

Where;

$$V_{py} = M_{py}\cdot a_{py} \quad \text{with} \quad a_{py} = \sqrt{\gamma R T_{py}} \tag{15}$$

$$V_{sy} = M_{sy}\cdot a_{sy} \quad \text{with} \quad a_{sy} = \sqrt{\gamma R T_{sy}} \tag{16}$$

$$M_m = \frac{V_m}{a_m} \quad \text{with } a_m = \sqrt{\gamma R T_m} \tag{17}$$

Flow mixed from section m to section 3

$$\frac{P_3}{P_m} = 1+\frac{2\gamma}{\gamma+1}(M_m^2-1) \tag{18}$$

$$\frac{T_3}{T_m} = \left[1+\frac{2\gamma}{\gamma+1}(M_m^2-1)\right]\left[\frac{2+(\gamma-1)M_m^2}{(\gamma+1)M_m^2}\right] \tag{19}$$

$$M_3^2 = \frac{1+\frac{\gamma-1}{2}M_m^2}{\gamma M_m^2 - \frac{\gamma-1}{2}} \tag{20}$$

Flow mixed in the diffuser

$$\frac{T_c}{T_3} = 1+\frac{\gamma-1}{2}M_3^2 \tag{21}$$

$$\frac{p_c}{p_3} = (1+\frac{\gamma-1}{2}M_3^2)^{\frac{\gamma}{\gamma-1}} \tag{22}$$

Performance parameters

$$\omega = \frac{\dot{m}_s}{\dot{m}_p} \tag{23}$$

$$\dot{Q}_{ev} = \dot{m}_s(h_1 - h_4) \tag{24}$$

$$\dot{Q}_{co} = \dot{m}_s(h_{2-c} - h_3) \tag{25}$$

$$COP = \frac{\dot{Q}_{ev}}{GA} \tag{26}$$

$$COP_{overall} = COP\cdot\omega \tag{27}$$

4. THERMOECONOMIC STUDY

The thermoeconomic analysis allows to compare thermodynamic systems evaluating the product cost by using exergoeconomic balances for each component. The main aim is the comparison between an ejection cooling system driven by CPV module (CPV/ECS) and a traditional electric heat pump (EHP). This analysis is applied to a typical Southern Italy house of about 80 m^2 with demand of about 400 hours of summer conditioning and cooling load of 25 W/m^3. The same input data in terms of indoor (22°C) and outdoor (32°C) temperatures and cooling load, are considered in the comparison. As for the EHP, the refrigerant fluid is R444B [31], the compressor electric efficiency is 0.90, the isentropic efficiency is 0.75 and the superheating and undercooling degrees are equal to 5°C. Referring to the CPV/ECS, in the thermoeconomic analysis the CPV collector circuit and the generator are considered as a single component defined "thermal motor" included between the states 6 and g (Figure 1). The entrainment ratio value allows to evaluate powers, partial and total mass flow rates; the collector efficiency (η_{th}, η_{el}), $COP_{CPV/ES}$, $\dot{Q}_{ev}$ and solar irradiation values allow to determine the necessary PV surface. The exergoeconomic balances of the heat exchangers, both for EHP and CPV/ECS, have been adapted from [32]

where the concept of exergy, representing the maximum work obtainable from the system as it transitions from a specific to dead state interacting with environment, is defined.

condenser

$$C_2\dot{E}x_2 + \dot{Z}_{co} = C_3\dot{E}x_3 \quad (a)$$

evaporator

$$C_4\dot{E}x_4 + \dot{Z}_{ev} = C_1\dot{E}x_{1e} + C_{prod}\dot{E}x^{\dot{Q}ev} \quad (b)$$

Referring to EHP compressor:

compressor

$$C_1\dot{E}x_1 + C_L\dot{L}_c + \dot{Z}_c = C_2\dot{E}x_2 \quad (c)$$

As for the ejector the equation is:

Ejector:

$$C_1\dot{E}x_{1e} + C_g\dot{E}x_g + \dot{Z}_{eiet} + \dot{Z}_{coll} = C_2\dot{E}x_{2c} \quad (d)$$

where $\dot{Z}_{coll}$ is a cost that considerably affects the final product. It is not relevant to consider the collector exergoeconomic balance, but only how the thermal power production cost influences the product cost. As for the valve, the exergy destroyed is negligible with respect to other components, and tòòhen the exergoeconomic balance is not considered. For both systems C_{prod} is the cost of the system product represented by refrigeration power. As for the EHP the unknowns are six: C_1, C_2, C_3, C_4, C_{prod}, C_L with three available equations (a,b and c); related to CPV/ECS the unknowns are six: C_1, C_2, C_3, C_4, C_{prod}, C_g with three available equations (a, b and d) and some auxiliary equations are necessary. Related to the EHP, in the state *1* the cost is supposed equal to zero (c_1=0) and the compression costs increase is related only to state *2* (c_L=c_2). In the expansion valve there is not costs formation because the pressure decrease does not determine energy costs related to the refrigerant fluid (c_3=c_4); hence, three equations and three unknowns are available allowing a univocal solution. In the CPV/ECS the state *1e* is different from the state *2c* only for the additional cost related to *g* state (c_{1e}=c_{2c}), in the condenser the cost linked to heat exchange is considered equal to zero (c_3=c_{2c}) and in the expansion valve c_3=c_4; hence, the system allows a univocal solution.

5. RESULTS AND DISCUSSION

The model input data are outdoor temperature and solar irradiation of six sample Italian cities evaluated considering the position of each city according to latitude and longitude. As for solar cooling, it has been more useful to evaluate the monthly medium values of the maximum temperatures and solar irradiation. These values increase from north to south approaching the equator; the higher medium temperature (32.5°C) is reached at Palermo in August with a solar irradiation of 24.4 MJ/m^2; the minimum temperature (4.20°C) refers to Milano in January with solar irradiation of 5.51 MJ/m^2 (Figures 5 and 6). The collector model results are determined in terms of collector efficiency and working fluid temperature. In summer season the medium value of the thermal efficiency is about 0.55 (Figure 7). The working fluid heated by the CPV/T collector affects the ejector cooling system performances, heating in the generator the primary fluid that changes the compression ratio (Figure 8) and condenser inlet temperature values. In summer the generating temperatures determined are included in the range 90-95°C and in winter are often under 80°C (Figure 9).

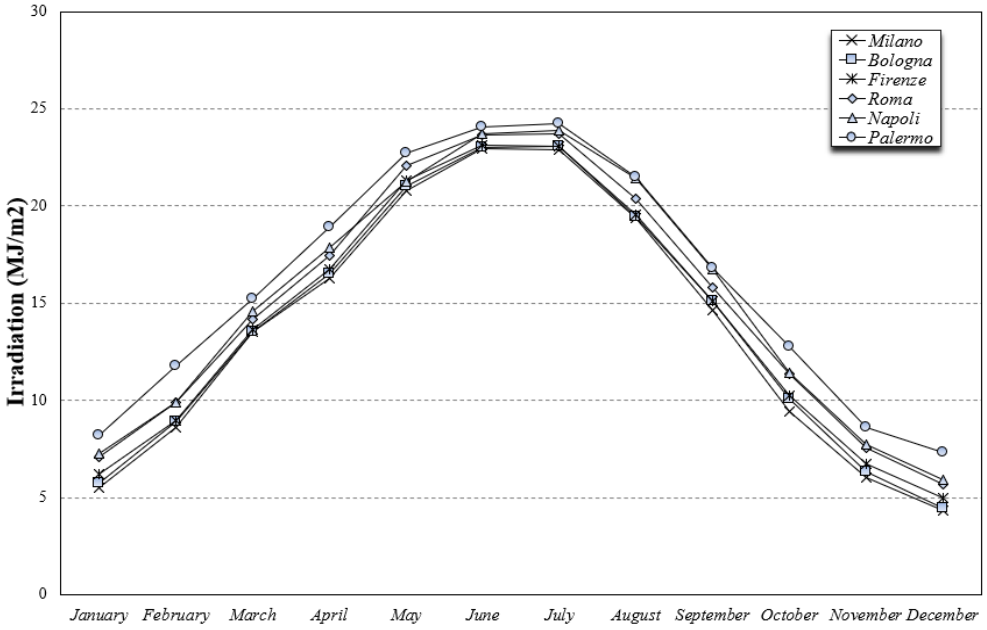

Fig. 5. Italian cities solar irradiation.

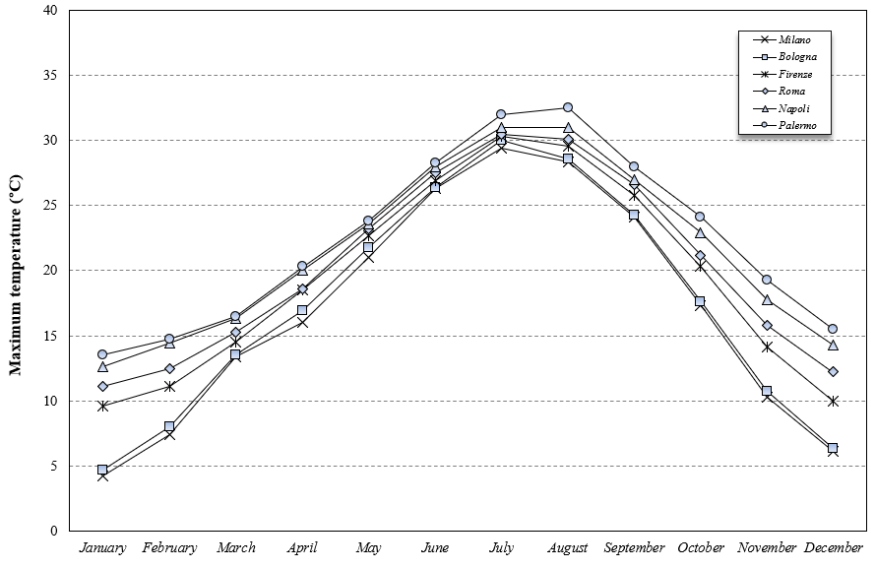

Fig. 6. Maximum temperature medium values of the Italian cities.

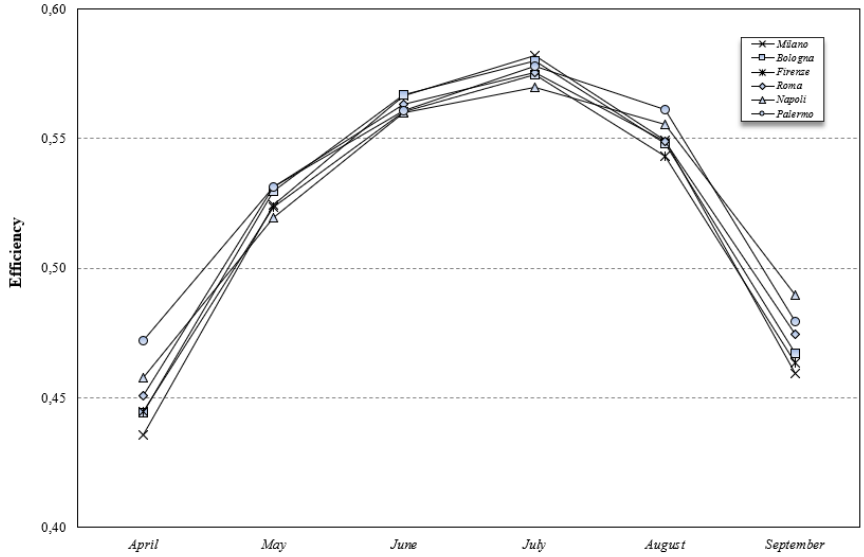

Fig. 7. Efficiency of the collector.

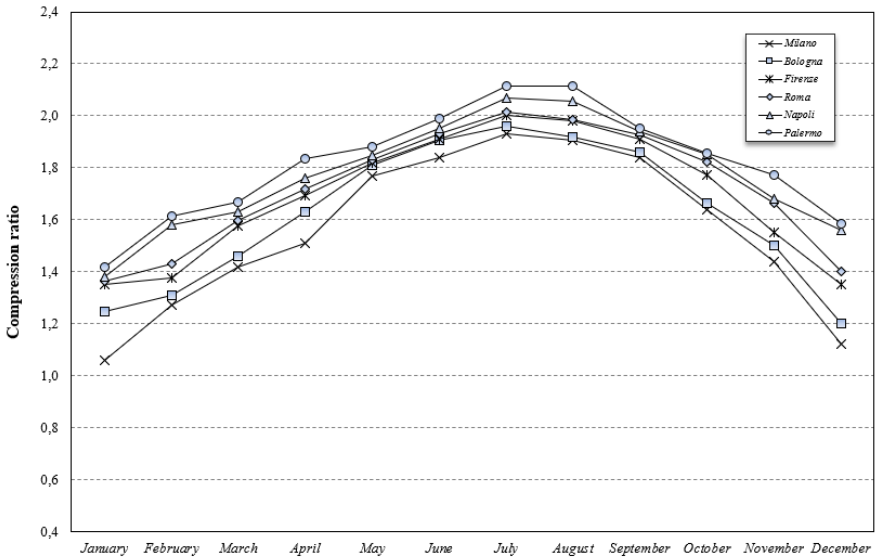

Fig. 8. Compression ratio.

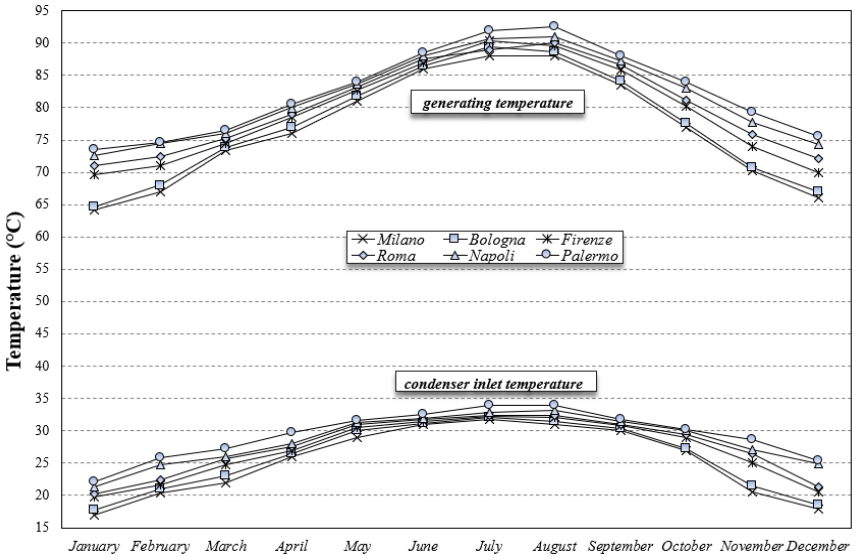

Fig. 9. Generating and condenser inlet temperatures.

To study the ejector model, it is necessary to define the temperature and pressure inlet values of the primary and secondary fluids; the primary fluid values are determined by means of the collector model, while the secondary fluid values are related to the evaporator outlet where the refrigerant fluid is generally in conditions of dry saturated vapour as reported in literature in many experimental tests [26], [30]. The model output data are the ejector entrainment ratio, the condenser input temperature, the secondary fluid mass flow rate and the cycle performances. The values are determined referring to the critical pressure limit that represents the working limit in double-choking. The model allows to determine the yearly ejector parameters for each city. In Figure 6 the condenser inlet temperature is reported; in the cold months the temperature values are under 30°C and the solar cooling is as little as possible. Hence, the model determines the entrainment ratio values only from April to September (Figure 8), and Palermo presents the best climatic conditions and performances. In the Figures 8 and 9 the $Q_{ev,}$ COP and $COP_{overall}$ values are reported referring to satisfactory entrainment ratio values. The model results show as the CPV/ECS system can be a good solution for air-conditioning in the hot months related to all Italian cities, but with higher performances in terms of evaporation power and COP in Southern Italy. The theoretical model results have been also compared in the same working conditions with the experimental data present in literature. In particular, the model has been also made to run under the same working conditions of the experimental tests realized in [11], where the ejector diameters d_3, d_t, and d_{p1} are equal respectively to 8.10 mm, 2.64 mm and 4.50 mm, and the generating temperature and condenser inlet temperature values are included respectively in the ranges 78-90°C and 30-34°C. Hence, entrainment ratio and COP values have been obtained by the model with a percentage deviation of about 4% from the experimental values [33]

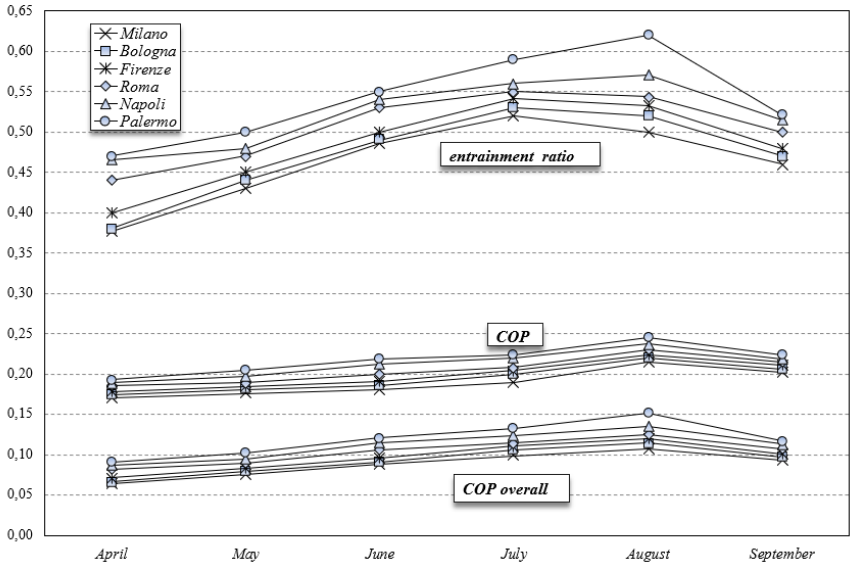

Fig. 10. Entrainment ratio, COP and $COP_{overall}$ values.

As for the thermoeconomic analysis, it is necessary first of all to determine the components cost and the plant working and maintenance costs. The components cost of the EHP is obtainable by means of catalogues or specific cost functions [33]. As for the operating cost, the annual costs of the compressor electric consumption have been considered [22].

Referring to the CPV/ECS, the collector cost is 3.3 €/W_p [20]; as for the ejector, condenser, evaporator, valve, tubes and generator, the costs are obtainable by means of catalogues or specific cost functions [35]. The maintenance costs are higher because, though the CPV systems use less silicon, they need major maintenance as they use optic lens [36]. In order to solve the equations system and to determine the product cost related to the EHP and CPV/ECS systems, it is necessary to calculate the $\dot{Z}$ values present in the exergoeconomic balances: $\dot{Z}_k = \frac{\dot{Z}^{PC} + \dot{Z}^{OM}}{\dot{Z}^{PC}_h} C_k$. The exergy destroyed cost of each component, equal to the product between $c_{i,k}$ at the component inlet with $\dot{Ex}_{d,k}$, represents the additional cost to supply to a component to meet the exergy destroyed. Hence, it is possible to determine the costs linked to different energetic fluxes, using the exergoeconomic balances with auxiliary relations, and then the hourly cost of each flux ($\dot{C}_k$) for both systems (Table 1). The product cost is 7.43 €/h for the EHP and 4.25 €/h for the CPV/ECS. So, EHP presents a higher value of exergy destroyed respect to the ejector system, but even if the CPV/ECS presents a higher investment cost, it allows to obtain a lower product cost respect to the EHP. The SPB has been calculated as ratio between the extra cost of the ejector system, and the cash flows equal to the difference between the annual costs necessary to obtain the refrigeration power with EHP and CPV/ECS; a SPB of 7.4 years has been obtained. Moreover, by also using the electric energy from the CPV system to meet domestic electric requirements, further savings are possible, with an SPB equal to 5.2 years considering a mean annual electric consumption of 3000 kWh/year for a family four people. Finally, the CPV/ECS allows to obtain electric energy and summer cooling with an economic saving respect to the traditional system.

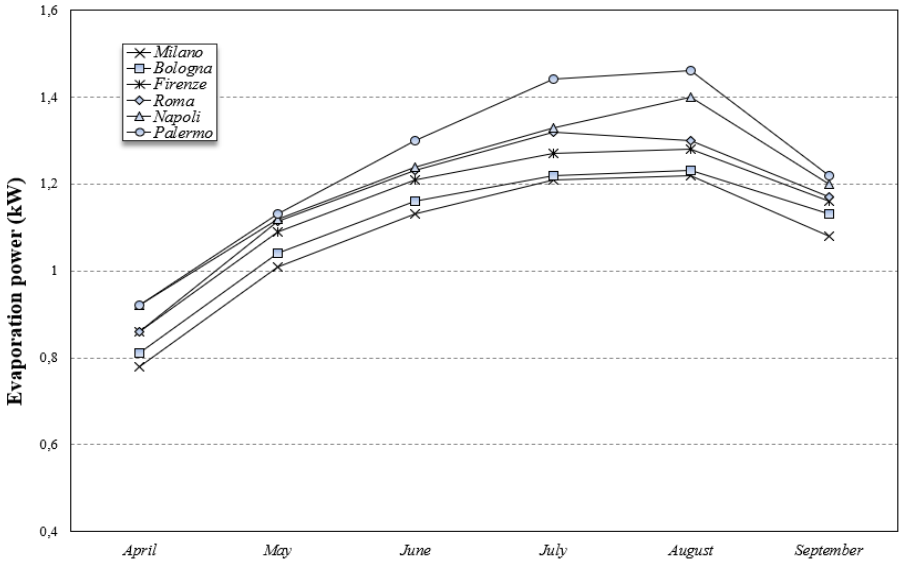

Fig. 11. Evaporator power.

Table 1. Exergoeconomic analysis results.

EHP	$c_{i,k}$ (€/kWh)	Ex (kW)	Ck (€/h)	CPV/ECS	$c_{i,k}$ (€/kWh)	Ex (kW)	Ck (€/h)
1	0	1.54	0	1e	7.49	1.52	11.4
2	1.83	2.64	4.83	2c	7.49	2.71	20.3
3	2.38	2.40	5.71	3	7.49	2.52	18.9
4	2.38	2.31	5.50	4	7.49	1.78	13.4
compressor	1.83	1.52	2.78	g	17.2	1.21	20.7
product	36.3	0.21	7.43	product	20.7	0.20	4.25

6. CONCLUSIONS

In this paper, the model of an ejector cooling system with CPV/T collector working in some Italian cities has been realized. The modelling has been developed with exemplifying hypotheses because of the complex fluid-dynamic phenomena. The model output data are collector efficiency, entrainment ratio, temperature and pressure values at the condenser inlet, evaporation power, COP and $COP_{overall}$. The ejector system works

better in Southern Italy cities where the climatic conditions are more favourable. The evaporation power is on average 1 kW/m^2 and the COP equal to about 0.25. The values of generating temperature, condenser inlet temperature and pressure, collector thermal efficiency and ejector entrainment ratio are respectively equal to 92.5°C, 34.5°C, 0.87 MPa, 0.58 and 0.62 in Palermo, whose values of temperature and solar irradiation are the highest among the Italian cities. An evaporation power of about 1.45 kW/m^2 has been obtained corresponding to an outdoor medium temperature of 32.5°C and a solar irradiation of 24.4 MJ/m^2. An ejector cooling system driven by a CPV/T collector is a good solution to satisfy the electric and cooling demands of the domestic applications. The model results are comparable with experimental data present in literature. Finally, it has been noted by means of the exergoeconomic analysis that the CPV/T module driven ejector cooling system, even if characterized by higher investment cost, allows lower product cost respect to a traditional cooling system together with possibility to produce electrical energy. In particular, a SPB of 7.4 years is obtained using a CPV/ECS system instead of traditional EHP and a further saving is possible, with SPB equal to 5.2 years, when also the electric requirements of a domestic user are satisfied by CPV/T system.

NOMENCLATURE

Symbols

A	area, m^2
a	sonic velocity, m/s
$C_{i,k}$	cost for exergy unity, €/kWh
COP	coefficient of performance
c_p	constant pressure specific heat, kJ/kgK
C_{prod}	cost of the system product, €/kWh
c_v	constant volume specific heat, kJ/kgK
CPV	concentrating photovoltaic
CPV/T	concentrating photovoltaic/thermal
d	diameter, m
EHP	electric heat pump
$\dot{E}x_{d,k}$	exergy destroyed (kW)
ECS	ejection cooling system
G	solar irradiance, W/m^2
h	enthalpy, kJ/kg
M	Mach number
$\dot{m}$	mass flow rate, kg/s
P	pressure, MPa
PV	photovoltaic
$\dot{Q}$	Power, W
R	gas constant, kJ/kgK
SPB	simple pay-back
T	temperature, K; thermal
V	gas velocity, m/s
Z	cost, €

Greek symbols

γ	ratio $\frac{c_p}{c_v}$
η,	efficiency
ρ	density, kg/m^3
ω	entrainment ratio

Subscripts

1	nozzle outlet
2	constant area inlet section
3	constant area outlet section
c	ejector outlet
coll	collector
comp	compressor
cond	condensation
e	secondary fluid at ejector inlet
eiet	ejector
el	electric
ev	evaporation
g	primary fluid at ejector inlet (nozzle inlet)
inv	inverter
m	flow mixed
o	outdoor; static
op	optical
p	primary flux
par	parasitic
p_1	primary flux at nozzle outlet
pv	photovoltaic
p	primary flux at section y
rad	radiation
s	secondary flux
sy	secondary flux in efflux critical conditions
t	throat section of the nozzle
th	thermal
y	throat hypothetical section of the secondary fluid.

REFERENCES

[1] Wang C., Wu X., Sun S., Zhang Z., and Xing Z., 2022. Potential evaluation of water-cooled multiple screw chillers with serial water loops and development of ultra-efficient dual screw chillers. *Applied Thermal Engineering* 210: 118340.

[2] Kober T., Schiffer H.W., Densing M., and Panos E., 2020. Global energy perspectives to 2060–WEC's World Energy Scenarios 2019. *Energy Strategy Reviews* 31: 100523.

[3] González-Torres M., Pérez-Lombard L., Coronel J.F., Maestre I.R., and Yan D., 2022. A review on buildings energy information: Trends, end-uses, fuels and drivers. *Energy Reports* 8: 626-637.

[4] IEA, Reports. 2019. The future of cooling.

[5] Yadav V.K., Sarkar J., and Ghosh P., 2022. Thermodynamic, economic and environmental analyses of novel solar-powered ejector refrigeration systems. *Energy Conversion and Management* 264: 115730.

[6] Tashtoush B., Songa I., and Morosuk T., 2022. Exergo-economic analysis of a variable area solar ejector refrigeration system under warm weather conditions. *Energies* 15 (24): 9540.

[7] Besagni G., Mereu R., and Inzoli F., 2016. Ejector refrigeration: A comprehensive review. *Renewable and Sustainable Energy Reviews* 53: 373-407.

[8] Elakhdar M., Landoulsi H., Tashtoush B., Nehdi E., and Kairouani L., 2019. A combined thermal system of ejector refrigeration and organic Rankine

cycles for power generation using a solar parabolic trough. *Energy Conversion and Management* 199: 111947.

[9] Bejan A., Vargas J.V.C., and Sokolov M., 1995. Optimal allocation of a heat-exchanger inventory in heat driven refrigerators. *Int. J. Heat Mass Transfer* 38: 2997-3004.

[10] Yen R.H., Huang B.J., Chen C.Y., Shiu T.Y., Cheng C.W., Chen S.S., and Shestopalov K., 2013. Performance optimization for a variable throat ejector in a solar refrigeration system. *International Journal of Refrigeration* 36(5): 1512-1520.

[11] Huang B.J., Chang J.M., Petrenko V.A., and Zhuk K.B., 1998. A solar ejector cooling system using the refrigerant R141b. *Solar energy* 64: 223-226.

[12] Huang B.J., Ko H.W., Ton W.Z., Wu C.C., Chang H.S., Hsu H.Y., and Petrenko V.A., 2018. Modified solar-assisted ejector cooling system. *EuroSun 2018 Conference Proceedings.*

[13] Huang B.J., Chang J.M., Wang C.P., and Petrenko V.A., 1998. A 1-D analysis of ejector performance. *International Journal of Refrigeration* 22: 354-364.

[14] Nguyen V.M., Riffat S.B., and Doherty P.S., 2001. Development of a solar-powered passive ejector cooling system. *Applied Thermal Engineering* 21:157-168.

[15] Cheng Y., Wang M., and Yu J., 2021. Thermodynamic analysis of a novel solar-driven booster-assisted ejector refrigeration cycle. *Solar Energy* 218: 85-94.

[16] Abbady K., Al-Mutawa N. and Almutairi A., 2023. The performance analysis of a variable geometry ejector utilizing CFD and artificial neural network. *Energy Conversion and Management* 291: 117318.

[17] Chunnanond K. and S. Aphornratana. 2004. Ejectors: applications in refrigeration technology. *Renewable and Sustainable Energy Reviews* 8(2): 129-155.

[18] Braimakis K., 2021. Solar ejector cooling systems: A review. *Renewable Energy* 164: 566-602.

[19] Sornek K., Żołądek M., Papis-Frączek K., Szram M., and Filipowicz M., 2023. Experimental investigations of the microscale concentrated photovoltaic/thermal system based on a solar parabolic trough concentrator. *Energy Reports* 9: 86-97.

[20] Vignesh N., Arunachala U.C., and Varun K., 2023. Innovative conceptual approach in concentrated solar PV/thermal system using Fresnel lens as the concentrator. *Energy Sources, Part A: Recovery, Utilization, and Environmental Effects* 45(4): 10122-10143.

[21] Kribus A., Kaftori D., Mittelman G., Hirshfeld A., Flitsanov Y., and Dayan A., 2006. A miniature concentrating photovoltaic and thermal system. *Energy Conversion and Management* 47: 3582-3590.

[22] Abdulateef J.M., Sopian K., Alghoul M.A., and Sulaiman M.Y., 2009. Review on solar-driven ejector refrigeration technologies. *Renewable and Sustainable Energy Reviews* 13: 1338-1349.

[23] ENEA, The Italian National Agency for New Technologies, Energy and the Environment.

[24] Renno C., D'Agostino D., Minichiello F., Petito F., and Balen I., 2019. Performance analysis of a CPV/T-DC integrated system adopted for the energy requirements of a supermarket. *Applied Thermal Engineering* 149: 231-248.

[25] Wang X., Yan Y., Li B., Hao X., Gao N., and Chen G., 2020. Prospect of solar-driven ejector-compression hybrid refrigeration system with low GWP refrigerants in summer of Guangzhou and Beijing. *International Journal of Refrigeration* 117: 230-236.

[26] Renno C. and F. Petito. 2018. Triple-junction cell temperature evaluation in a CPV system by means of a Random-Forest model. *Energy Conversion and Management* 169: 124-136.

[27] Wang G., Wang F., Chen Z., Hu P., and Cao R., 2019. Experimental study and optical analysis of a multi-segment plate concentrator (MSP) for a concentrating solar photovoltaic (CPV) system. *Renewable Energy* 134: 284-291.

[28] Matlab R2023b, The MathWorks.

[29] REFPROP: Reference Fluid Thermodynamic and Transport Properties Database: Version 8.0, NIST.

[30] He S., Li Y., and Wang R.Z., 2009. Progress of mathematical modeling on ejectors. *Renewable and Sustainable Energy Reviews* 13: 1760-1780.

[31] Krajcik M., Straba D., Masaryk M., Sikula O., and Mlynàr P., 2022. Enanching the efficiency of a stram jet ejector chiller for chilled ceiling. *Applied Thermal Engineering* 211

[32] Sadeghi M., Mahmoudi S.M.S., and Saray K.R., 2015. Exergonomic analysis and multi-objective optimization of an ejector refrigeration cycle powered by an internal combustion (HCCI) engine. *Energy Conversion and Management* 96: 403-417.

[33] Wang J.H., Wu J.H., Hu S.S., and Huang B.J., 2009. Performance of ejector cooling system with thermal pumping effect using R141b and R365mfc. *Applied Thermal Engineering* 29: 1904-1912.

[34] Prabakaran R., Sivalingam V., Kim S.C., Ganesh Kumar P., and Praveen Kumar G., 2022. Future refrigerants with low global warming potential for residential air conditioning system: A thermodynamic analysis and MCDM tool optimization. *Environmental Science and Pollution Research* 29 (52): 78414-78428.

[35] El-Sayed Y., 1999. A short course in Thermo-economics, Summer School, Ovidius University, Constantza, Romania.

[36] Renno C., 2022. Comparison of the spherical optics and Fresnel lens performance in a point-focus CPV system. *International Energy Journal* 22: 1-12.